DISCRETE AND CONTINUOUS
DYNAMICAL SYSTEMS SERIES B
Volume **22**, Number **6**, August **2017**

doi:10.3934/dcdsb.2017095

pp. **2261–2290**

SEASONAL FORCING AND EXPONENTIAL THRESHOLD INCIDENCE IN CHOLERA DYNAMICS

Jinhuo Luo

College of Information Technology, Shanghai Ocean University
Shanghai 201306, China

Jin Wang

Department of Mathematics, University of Tennessee at Chattanooga
Chattanooga, TN 37403, United States

Hao Wang*

Department of Mathematical and Statistical Sciences, University of Alberta
Edmonton, AB T6G 2G1, Canada

(Communicated by Gail Wolkowicz)

Abstract. We propose a seasonal forcing iSIR (indirectly transmitted SIR) model with a modified incidence function, due to the fact that the seasonal fluctuations can be the main culprit for cholera outbreaks. For this nonautonomous system, we provide a sufficient condition for the persistence and the existence of a periodic solution. Furthermore, we provide a sufficient condition for the global stability of the periodic solution. Finally, we present some simulation examples for both autonomous and nonautonomous systems. Simulation results exhibit dynamical complexities, including the bistability of the autonomous system, an unexpected outbreak of cholera for the nonautonomous system, and possible outcomes induced by sudden weather events. Comparatively the nonautonomous system is more realistic in describing the indirect transmission of cholera. Our study reveals that the relative difference between the value of immunological threshold and the peak value of bacterial biomass is critical in determining the dynamical behaviors of the system.

1. **Introduction.** Cholera is a severe intestinal disease caused by ingesting water contaminated with the bacterium *Vibrio cholerae*. The main symptom of cholera infection is profuse watery diarrhea that rapidly causes dehydration and can lead to death within days if not promptly treated. Although listed as one of the oldest known diseases, cholera remains a serious public health burden in developing countries where poverty and poor sanitation and hygiene are prevalent. Major cholera outbreaks in recent years include those in Zimbabwe in 2008, Vietnam in 2009, Nigeria in 2010, Ghana in 2011, as well as the one in Haiti during 2010-2012 which is regarded as one of the largest cholera epidemics in modern history, with more than 530,000 reported cases and over 7,000 deaths [24].

2010 *Mathematics Subject Classification.* 93A30, 37B55, 34D20, 34D23, 97M10, 34C25, 37D35, 34C60.

Key words and phrases. Cholera, nonautonomous, stability, seasonal forcing, immunological threshold, persistence, periodic solution, exponential incidence, sudden events.

The second author's research was partially supported by NSF.

*Corresponding author. The third author's research was partially supported by NSERC.

Mathematical models for infectious disease transmission play an important role in understanding the disease persistence (endemic) and outbreaks (epidemic, pandemic), and can provide useful insights toward effective prevention and control of disease spread. In particular, a number of mathematical models for cholera have been proposed and analyzed in recent years [4, 8, 13, 12, 18, 10, 22, 19, 1, 2, 20, 3, 11], and several models have been driven by the Haiti cholera outbreak [1, 2, 3, 20]. These studies have certainly made significant contribution to cholera epidemiology. Nevertheless, the persistence of cholera nowadays and its frequent outbreaks throughout the world indicate that our current knowledge in cholera dynamics and public health guidelines to control the disease are still inadequate.

Since cholera is a water-borne disease, recent mathematical cholera models have extended the classical SIR (susceptible-infected-recovered) framework by adding an environmental component, typically denoted by B, that tracks the concentration of toxigenic vibrios in the water supply. Particularly, Codeço [4] published a cholera model that, in the first time, explicitly incorporated the pathogen concentration, with the infection from the aquatic environment represented by a saturation incidence. Codeço's model has since been extensively referenced, discussed, and improved (see, e.g., [8, 10, 13, 22, 18, 19]). Most of these studies, however, assume a simple linear representation of the pathogen dynamics, and the rate of change for the bacterial concentration is typically described by two linear factors: a positive contribution from the infected human population, and a negative contribution due to natural death of the vibrios. Joh et al. in 2009 proposed a model [10] that took into account the intrinsic growth of the vibrios in the aquatic environment, and a logistic growth term was included in their model to depict the bacterial dynamics. Meanwhile, the model of Joh et al. introduced a minimal infection dose (MID) in the incidence term, based on clinical observations [14] that cholera infection takes place only if the concentration of the ingested vibrios is high enough to overcome the innate immune response of human body. Thus, an infection threshold is imposed by this MID and the incidence function is piecewise continuous: it is zero if the vibrio concentration is below the threshold, and it is a Holling type functional response if the vibrio concentration is above the threshold.

The present paper is built upon the framework of Joh et al.. As mentioned above, the incidence in [10] is a piecewise continuous function which exhibits a discontinuity for higher order derivatives. In this study, we will introduce a new and first-of-its-kind representation of the incidence which is infinitely smooth, by replacing the Holling type function with an exponential saturation form. Our proposed incidence function matches very well in values (thus biologically mimics) the standard Holling type II or III function, yet the new incidence form possesses better mathematical properties that allows us to conduct a careful analysis on the rich dynamics resulting from the MID threshold.

The main objective of this paper is to investigate the effects of seasonal forcing on cholera epidemics and endemism. Particularly, we examine the seasonality of bacterial growth which is subject to the annual variation of temperature, nutrients, rainfall, etc. [6, 17]. Such periodic oscillations of bacterial growth and decay, in turn, have strong impact on short- and long-term cholera dynamics. We extend our autonomous cholera model into a nonautonomous system with periodic bacterial growth rate and carrying capacity, and rigorously analyze the dynamics. In particular, we prove the persistence of the disease and the existence of periodic solutions under mild assumptions.

The remainder of this paper is organized as follows. In Section 2, we introduce the new exponential saturation incidence and incorporate periodicity into the iSIR model. In Section 3, we provide the forward invariance, the uniform persistence, the existence and stability (local and global) of periodic solutions, for the nonautonomous system. In Section 4, we conduct numerical simulations to validate the analytical results and to test the impact of sudden weather events on cholera outbreaks. Finally, we summarize and discuss our conclusions in Section 5.

2. **Model derivation.** The autonomous iSIR model was introduced in [10]:

$$\begin{cases} \dfrac{dS}{dt} = & -\alpha(B)S - \mu S + \mu N \ , & \text{(1a)} \\ \dfrac{dI}{dt} = & \alpha(B)S - \mu I - \delta I \ , & \text{(1b)} \\ \dfrac{dR}{dt} = & \delta I - \mu R \ , & \text{(1c)} \\ \dfrac{dB}{dt} = & rB(1 - \frac{B}{K}) + \xi I \ , & \text{(1d)} \end{cases}$$

where the saturation function $\alpha(B)$ takes the form as follows:

$$\alpha(B) = \begin{cases} 0 \ , & B \le c \\ \frac{a(B-c)^n}{(B-c)^n + H^n}, & B > c \end{cases} \text{, where n is a positive integer.} \qquad (2)$$

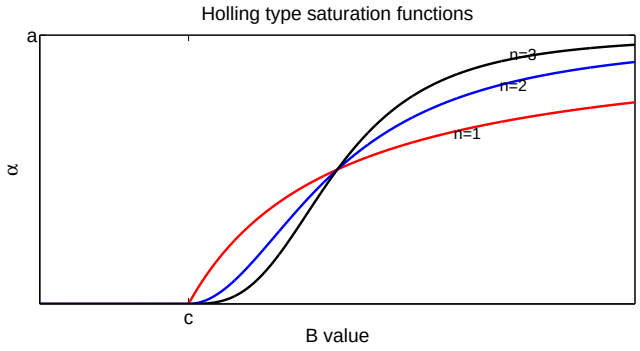

FIGURE 1. Satuation function $\alpha(\cdot)$ of Holling-type

Although as n becomes larger, the curve will become smoother, these curves are not sufficiently smooth, posing challenges in mathematical analysis. we thus introduce the following novel exponential threshold incidence function which is infinitely smooth:

$$\alpha(B) = \begin{cases} 0 \ , & B \le c \\ a \exp(-\frac{H^n \ln 2}{(B-c)^n}), & B > c \end{cases} \text{, where n is a positive number.} \qquad (3)$$

Obviously this new function satisfies the half saturation condition (when $B-c = H$, we have $\alpha(B) = a/2$).

In addition, we define the value of the i-th derivative of $\alpha(\cdot)$ at c as 0 for $i = 1, 2, \cdots$. It is easy to show that for every positive number n, the function $\alpha(\cdot)$ is infinitely smooth. The advantage of such defined functions is reflected not only in

theoretical analysis but also in numerical simulations. We will highlight this point throughout the paper.

To our knowledge, such an exponential threshold incidence from is first of its kind. It is clear from Figures 1 and 2 that these exponential functions match corresponding Holling type functions very well, yet with better mathematical properties that enable us to deepen our understanding of the rich dynamics of the cholera model. In addition, these exponential saturation functions can be potentially applied to the modeling of many other infectious diseases where the minimal infection doses (MID) are relevant. For these reasons, we carefully analyze the exponential incidence incorporated in system (1), under a relatively simple, autonomous setting; the details are provided in Appendices. The global stability analysis repeats almost the same process in Kong et al. [11], thus we do not present global results here. The results of the autonomous system build a solid base for our mathematical analysis of the more complex, nonautonomous system in Section 3.

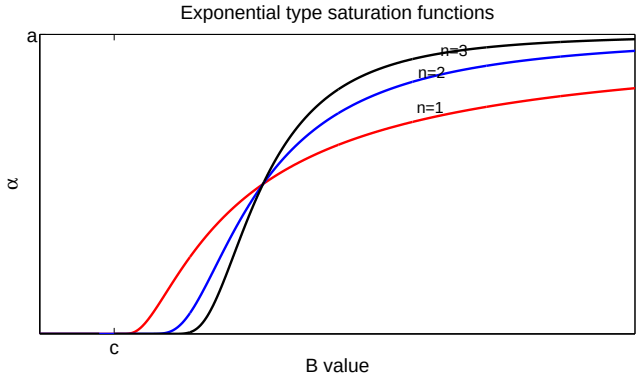

FIGURE 2. Saturation function $\alpha(\cdot)$ of exponential type

The parameters in system (1) are described in Table 1, taken from Jensen et al. [9].

TABLE 1. Parameter values from Jensen et al. [9]

Parameter	Values	Description	Units
r	0.2-14.3	Maximum per capita pathogen growth rate	day $^{-1}$
K	10^6	Pathogen carrying capacity	cell liter $^{-1}$
H	$10^6 - 10^8$	Half-saturation pathogen density	cell liter $^{-1}$
a	0.08 - 0.12	Maximum rate of infection	day $^{-1}$
δ	0.1	Recovery rate	day $^{-1}$
ξ	10-100	Pathengen shed rate	cell liter $^{-1}$day^{-1}
μ	$5 \times 10^{-5} - 5 \times 10^{-4}$	Natural human birth/death rate	day $^{-1}$
N	10^6	Total Population	persons
c	$\approx 10^6$	Minimum infection dose	cell liter $^{-1}$

Seasonal forcing is believed to be an important culprit for cholera outbreaks due to the indirect transmission from the reservoir that heavily depends on weather events. Here we explicitly incorporate seasonality into the bacterial intrinsic growth

rate and carrying capacity in our iSIR model, and obtain

$$\begin{cases} \frac{dS}{dt} = & -\alpha(B)S - \mu S + \mu N, & (4a) \\ \frac{dI}{dt} = & \alpha(B)S - \mu I - \delta I, & (4b) \\ \frac{dR}{dt} = & \delta I - \mu R, & (4c) \\ \frac{dB}{dt} = & r(t)B(1 - \frac{B}{K(t)}) + \xi I, & (4d) \end{cases}$$

where $\alpha(B)$ takes the exponential threshold form of (3), and S, I, R satisfy $S + I + R = N$.

We assume $r(t)$ and $K(t)$ are all positive continuous periodic functions, i.e., there exist ω, r_m, r_M, K_m, and K_M such that $r(t+\omega) = r(t), K(t+\omega) = K(t)$, and

$$0 < r_m \le r(t) \le r_M, 0 < K_m \le K(t) \le K_M.$$

For simplicity, we set $s = S/N, i = I/N$, and drop equation(4c). We rewrite system (4) in an equivalent form as

$$\begin{cases} \frac{ds}{dt} = & -\alpha(B)s - \mu s + \mu, & (5a) \\ \frac{di}{dt} = & \alpha(B)s - \mu i - \delta i, & (5b) \\ \frac{dB}{dt} = & r(t)B(1 - \frac{B}{K(t)}) + \xi N i. & (5c) \end{cases}$$

3. Mathematical analysis.

3.1. Forward invariance.

Proposition 3.1. *There exists $B_M > 0$, such that system (5) has a forward invariant set*

$$D_1 = \{(s, i, B) | s \ge \varepsilon_1,\ i \ge 0,\ \varepsilon_1 \le s + i \le 1,\ K_m \le B \le B_M\}.$$

Proof. Taking $\varepsilon_1 = \frac{\mu}{a+\mu}$. The condition $s \le \varepsilon_1$ implies $s \le \frac{\mu}{\alpha(B)+\mu}$. By (5a), if $s \le \varepsilon_1$, then $\dot{s} \ge 0$; by (5b), if $i = 0$, then $\dot{i} \ge 0$; and by (5c), if $B \le K_m$ then $\dot{B} \ge 0$. Hence we have $s(t) > \varepsilon_1$ and $i(t) \ge 0$ and $B(t) \ge K_m$ for $t > 0$ provided $(s(0), i(0), B(0)) \in D_1$.

According to (5a) and (5b), we have

$$\frac{d(s+i)}{dt} = -\mu(s+i) + \mu - \delta i.$$

If $s + i = 1$, then $\frac{d(s+i)}{dt} = -\delta i \le 0$. Hence we have $s(t) + i(t) \le 1$ for $t > 0$.

Note that $B \ge \frac{K_M + \sqrt{K_M^2 + 4K_M N\xi/r_m}}{2}$ implies $B^2 - K_M B - K_M N\xi/r_m \ge 0$, and thus it implies $\frac{dB}{dt} = r(t)B(1 - \frac{B}{K(t)}) + N\xi i \le 0$. Set $B_M = \frac{K_M + \sqrt{K_M^2 + 4K_M N\xi/r_m}}{2}$, then $B \ge B_M$ implies $\frac{dB}{dt} \le 0$. Hence for any initial value $(s_0, i_0, B_0) \in D_1$, we have $(s(t), i(t), B(t)) \in D_1$ for $t > 0$. This completes the proof. □

3.2. **Persistence.** We proceed to show the uniform persistence of the system (5). To that end, we first establish the following result.

Theorem 3.2. *Suppose there exist a number $L > 0$, a number $l, 0 < l < L$, and an $\varepsilon_0 > 0$, such that for every $t > 0$, there is an interval J of length l, $J \subseteq [t,\ t+L]$, and for every $\tau \in J$,*

$$B(\tau) \geq c + \varepsilon_0 \tag{6}$$

holds. Then there exist $\varepsilon_1 > 0, \varepsilon_2 > 0$, and $\varepsilon_3 > 0$ such that for every positive solution $(s(t),\ i(t),\ B(t))$ of system (5) satisfying (6), we have

$$\lim_{t\to+\infty} \inf s(t) \geq \varepsilon_1 > 0, \tag{7}$$

$$\lim_{t\to\infty} \inf i(t) \geq\ \varepsilon_2 > 0, \tag{8}$$

and

$$\lim_{t\to\infty} \sup\,(s(t) + i(t)) \leq\ \varepsilon_3 < 1. \tag{9}$$

Proof. By (6), there exists an $A > 0$ such that

$$\int_t^{t+L} \alpha(B(\tau))d\tau \geq A > 0,\ \text{for}\ \forall\, t > 0. \tag{10}$$

According to (5a) and $\alpha(B) \leq a$, we have

$$\frac{ds}{dt} \geq -as - \mu s + \mu. \tag{11}$$

Since the equation

$$\frac{du}{dt} = -au - \mu u + \mu \tag{12}$$

possesses a globally stable solution $u = \frac{\mu}{a+\mu}$, comparing the two equations (11) and (12), we have

$$\lim_{t\to\infty} \inf s(t) \geq \frac{\mu}{a+\mu}.$$

Set $\varepsilon_1 = \frac{\mu}{a+\mu}$, and we obtain (7).

Picking μ_1 such that $0 < \mu_1 < \varepsilon_1$, then there exists a $T_1 > 0$ such that

$$s(t) \geq \mu_1, \quad \text{for}\ t \geq T_1. \tag{13}$$

By (5b), we have

$$\frac{di}{dt} + (\mu + \delta)i \geq \mu_1\alpha(B), \quad \text{for} \quad t \geq T_1. \tag{14}$$

It follows

$$\frac{d(i\exp((\mu+\delta)t))}{dt} \geq \mu_1 \exp((\mu+\delta)t)\alpha(B), \quad \text{for} \quad t \geq T_1. \tag{15}$$

Integrating both sides over $[T_1,\ T]$, we get

$$i(T)\exp((\mu+\delta)T) - i(T_1)\exp((\mu+\delta)T_1) \geq \mu_1 \int_{T_1}^{T} \exp((\mu+\delta)t)\alpha(B(t))dt.$$

Hence we have

$$i(T) \geq i(T_1)\exp((\mu+\delta)(T_1 - T)) + \mu_1 \frac{\int_{T_1}^{T} \exp((\mu+\delta)t)\alpha(B(t))dt}{\exp((\mu+\delta)T)} \triangleq i_1(T) + i_2(T) \tag{16}$$

Obviously

$$\lim_{T\to+\infty} i_1(T) = 0. \tag{17}$$

Let $T = T_1 + nL + \Delta T$, where $0 \le \Delta T < L$ and n is a non-negative integer. Considering (10), we have

$$i_2(T) = \mu_1 \frac{(\int_{T_1}^{T_1+L} + \int_{T_1+L}^{T_1+2L} + \cdots + \int_{T_1+(n-1)L}^{T_1+nL} + \int_{T_1+nL}^{T_1+nL+\Delta T}) \exp((\mu+\delta)t)\alpha(B(t))dt}{\exp((\mu+\delta)nL)\exp((\mu+\delta)(T_1+\Delta T))}$$

$$\ge \mu_1 \frac{\exp((\mu+\delta)T_1)(1+\exp(L(\mu+\delta)) + \exp(2L(\mu+\delta)) + \cdots + \exp((n-1)L(\mu+\delta)))A}{\exp((\mu+\delta)nL)\exp((\mu+\delta)(T_1+\Delta T))}$$

$$\ge \frac{\mu_1 A}{\exp((\mu+\delta)(n+1)L)} \frac{\exp(nL(\mu+\delta))-1}{\exp(L(\mu+\delta))-1}.$$

Hence

$$\lim_{T\to+\infty} \inf i_2(T) \ge \lim_{n\to+\infty} \frac{\mu_1 A}{\exp((\mu+\delta)(n+1)L)} \frac{\exp(nL(\mu+\delta))-1}{\exp(L(\mu+\delta))-1} = \frac{\mu_1 A}{\exp(2L(\mu+\delta))}$$

Taking

$$\varepsilon_2 = \frac{\mu_1 A}{\exp(2L(\mu+\delta))}, \tag{18}$$

due to (16) and (17), we have

$$\lim_{T\to+\infty} \inf i(T) \ge \lim_{T\to+\infty} \inf (i_1(T) + i_2(T)) \ge \varepsilon_2.$$

Now by (8), there exists a $T_2 > 0$ such that

$$i(t) \ge \frac{\varepsilon_2}{2}, \quad \text{for } \forall t \ge T_2,$$

thus by (4c) we have

$$\frac{dR}{dt} \ge N\delta\frac{\varepsilon_2}{2} - \mu R, \quad \text{for } t \ge T_2. \tag{19}$$

Consider

$$\frac{dv}{dt} = N\delta\frac{\varepsilon_2}{2} - \mu v. \tag{20}$$

It has a solution $v = \frac{N\delta\varepsilon_2}{2\mu}$ which is globally stable. Based on (19) and (20), by the comparison theorem [23], we have

$$\lim_{t\to+\infty} \inf R(t) \ge N\frac{\delta\varepsilon_2}{2\mu} > 0,$$

which implies (9). □

Remark 3.3. Obviously, (7),(8) and (9) imply the persistence of (4). The hypothesis of this theorem has a reasonable background in reality. For example, if for every year there is a period, even if very short, within which the bacterial density is higher than the threshold value c, then the infection will spread and the disease will persist.

The hypothesis can also be given in another form. Consider the equation

$$\frac{dB}{dt} = r(t)B(1 - \frac{B}{K(t)}), \tag{21}$$

where $r(t)$, $K(t)$ are positive continuous ω-periodic functions. It can be shown that this equation possesses a unique periodic solution $\tilde{B}$, which is globally asymptotically stable. Specifically, we have the following result.

Lemma 3.4. *The system (21) has a positive ω-periodic solution $\tilde{B}(t)$, given by*

$$\tilde{B}(t) = \frac{1 - exp(-\int_0^\omega r(\theta)d\theta)}{\int_0^\omega \frac{r(t-\theta)}{k(t-\theta)} exp(-\int_0^\theta r(t-\tau)d\tau)d\theta}, \tag{22}$$

where $r(t)$, $K(t)$ are positive ω-periodic functions.

According to (5c) and (21), by the comparison theorem [23] we know that for any solution of system (5), $(s(t),\ i(t),\ B(t))$ with positive initial values, there must exist a $T > 0$ such that

$$B(t) > \tilde{B}(t), \quad \text{for } t > T.$$

Hence, we have

Theorem 3.5. *Assume that $c < \max_{t\in[0,\omega]} \tilde{B}$, where $\tilde{B}$ is given by (22). Then the system (4) is uniformly persistent, i.e., there exists a positive constant ε such that for all initial values $(S(0), I(0), R(0), B(0)) \in R^+ \times R^+ \times R^+ \times R^+$, we have $\lim_{t\to+\infty} \inf(S(t), I(t), R(t), B(t)) \geq (\varepsilon,\ \varepsilon,\ \varepsilon,\ \varepsilon)$.*

Proof. Taking $L = \omega,\ \varepsilon = \min\{\varepsilon_1, \varepsilon_2, 1-\varepsilon_3, K_m\}$, the assumption $c < \max_{t\in[0,\omega]} \tilde{B}$ implies (10), and the remaining proof follows the same logic as the proof of theorem (3.2). □

Furthermore, with the same assumption as in Theorem (3.5), we can establish the existence of positive periodic solutions.

Theorem 3.6. *In case of $c < \max_{t\in[0,\omega]} \tilde{B}$, system (5) possesses a periodic solution $(s^*(t), i^*(t), B^*(t))$ satisfying $(s^*(t), i^*(t), B^*(t)) > 0$, for $t \geq 0$.*

Proof. According to proposition (3.1),

$$D_1 = \{(s, i, B) | s \geq \varepsilon_1,\ i \geq 0,\ \varepsilon_1 \leq s + i \leq 1,\ K_m \leq B \leq B_M\}$$

is forward invariant. Since s, i and B are all bounded, obviously the periodic system (5) satisfies Lipschitz condition with the Lipschitz constant independent of t and system parameters. Hence, for every initial value $z_0 = (s(0), i(0), B(0)) \in D_1$, there exists an unique solution $z(t) \equiv (s(t), i(t), B(t))$. Denote $\varphi_{z_0}(t) = (z(t); 0, z(0))$ then $\varphi_{z_0}(t)$ is continuous with respect to z_0 for every $t > 0$. Define a map $T : D_1 \to D_1,\ T(z_0) = z(\omega)$, for $\forall\ z_0 \in D_1$ (Note that D_1 is invariant, which guarantees $z(\omega) \in D_1$). Since D_1 is a convex set and T is continuous, according to the fix point theorem, there must be at least one point $z_0^* = (s_0^*,\ i_0^*,\ B_0^*) \in D_1$, satisfying $z_0^* = z^*(\omega)$. Denote $\hat{z}(t) = z^*(t+\omega)$. Since $z^*(t)$ is a solution of system (5), obviously $\hat{z}(t)$ is also a solution of system (5). With $z^*(0) = \hat{z}(0)$, we have $z^*(t) \equiv \hat{z}(t)$ for $t \geq 0$. It means that $z^*(t) \equiv z^*(t + \omega)$. This proves the existence of the periodic solution for system (5). Now by the assumption $c < \max_{t\in[0,\omega]} \tilde{B}$, and the conclusion proved in theorem (3.2), we have

$$i_0^* = i^*(0) = i^*(\omega) = i^*(2\omega) = \cdots = \lim_{n\longrightarrow\infty} i^*(n\omega) \geq \varepsilon_2 > 0.$$

Hence the periodic solution z^* is positive. □

3.3. **Stability.** Generally speaking, stability analysis of non-autonomous dynamical systems is challenging. In what follows, we attempt to study the trivial and non-trivial periodic solutions of our model (5) under some stronger conditions.

We first present a known result below that characterizes the stability relationship between the trivial solution of a nonlinear system and that of the corresponding linear system[7][21].

Lemma 3.7. *Consider the system*

$$\frac{dX}{dt} = A(t)X + F(t,X), \tag{23}$$

where $F(t,X)$ is Lipschitzian in X for $\forall\, t$. Assume that

$$\lim_{|X|\to 0} \frac{|F(t,X)|}{|X|} = 0 \quad \textit{uniformly in } t.$$

(a) If $X=0$ is uniformly asymptotically stable for

$$\frac{dX}{dt} = A(t)X, \tag{24}$$

then $X=0$ is uniformly asymptotically stable for system (23).

(b) If $X=0$ is unstable for system(24), then $X=0$ is unstable for system (23).

We apply this lemma to system (5), and discuss two cases separately.

Case 1. Consider the disease-free and bacteria-free solution of the non-autonomous system (5): $(s,i,B)=(1,0,0)$. We transit this solution to the origin $X=0$ by introducing $y=1-s$, where $0\le\ y\le\ 1$. Then we have

$$\begin{cases} \dfrac{dy}{dt} = & -\mu y + \alpha(B)(1-y)\ , \\ \dfrac{di}{dt} = & -(\mu+\delta)i + \alpha(B)(1-y)\ , \\ \dfrac{dB}{dt} = & r(t)B + \xi N i - \frac{r(t)}{K(t)}B^2\ , \end{cases}$$

where

$$A(t) = \begin{bmatrix} -\mu & 0 & 0 \\ 0 & -(\mu+\delta) & 0 \\ 0 & \xi N & r(t) \end{bmatrix} \quad \text{and} \quad F(t,X) = \begin{bmatrix} \alpha(B)(1-y) \\ \alpha(B)(1-y) \\ -\frac{r(t)}{K(t)}B^2 \end{bmatrix}.$$

Clearly,

$$\begin{aligned} |F(t,X)|_\infty &\le 2\alpha(B)|1-y| + \tfrac{r(t)}{K(t)}B^2 \\ &\le \tfrac{r_M}{K_m}B^2, \quad \text{when } 0\le B<c, \quad \text{and} \\ |X|_\infty &\ge B. \end{aligned}$$

Here $|\cdot|_\infty$ represents the infinity norm.

$$\text{Thus} \quad \frac{|F(t,X)|_\infty}{|X|_\infty} \longrightarrow 0, \ \text{ as } \ |X|_\infty \longrightarrow 0, \ \text{uniformly in } t.$$

Now, the three Floquet exponents of system (24) are given by $-\mu$, $-(\mu+\delta)$ and $\frac{1}{\omega}\int_0^\omega r(t)dt > 0$. Thus its trivial solution $X=0$ is unstable. Based on the above lemma, we have

Theorem 3.8. *System (5) possesses a disease-free and bacteria-free trivial periodic solution* $(s,\ i,\ B) = (1,\ 0,\ 0)$*, which is unstable.*

Case 2. Consider $i = 0,\ B \neq\ 0$. It is stated for equation (21) that there exists an unique solution $\tilde{B}(t)$. Assume $\max_{t\in[0,\omega]} \tilde{B}(t) \leq c$, then we have an unique solution for system (5): $(s,\ i,\ B) = (1,\ 0,\ \tilde{B}(t))$. Let $y = 1 - s,\ z = \tilde{B} - B,$ then system (5) becomes

$$\begin{cases} \dfrac{dy}{dt} = & -\mu y + \alpha(\tilde{B} - z)(1 - y)\ , \\ \dfrac{di}{dt} = & -(\mu + \delta)i + \alpha(\tilde{B} - z)(1 - y)\ , \\ \dfrac{dz}{dt} = & \left(1 - \frac{2\tilde{B}(t)}{K(t)}\right) r(t)z - \xi N i + \frac{r(t)}{K(t)} z^2. \end{cases}$$

In this case we have

$$A(t) = \begin{bmatrix} -\mu & 0 & 0 \\ 0 & -(\mu + \delta) & 0 \\ 0 & -\xi N & \left(1 - \frac{2\tilde{B}(t)}{K(t)}\right) \end{bmatrix}.$$

Note that $\max_{t\in[0,\omega]} \tilde{B} \leq c$ and $\alpha(\tilde{B} - z) \longrightarrow 0$ exponentially as $z \longrightarrow 0$, again it can be easily shown that

$$\frac{|F(t, X)|_\infty}{|X|_\infty} \longrightarrow 0, \ \text{ as } \ |X|_\infty \longrightarrow 0, \ \text{uniformly in } t.$$

Hence the stability depends on the sign of the third Floquet exponent

$$\lambda_3 = \frac{1}{\omega} \int_0^\omega \left(1 - \frac{2\tilde{B}(t)}{K(t)}\right) r(t)dt.$$

Now we will show that $\lambda_3 < 0$. By the definition of $\tilde{B}(t)$ we simply have

$$\frac{d\tilde{B}}{dt} = r(t)\tilde{B}(1 - \frac{\tilde{B}}{K(t)}).$$

Obviously $\tilde{B}(t) \neq 0$ for $t \in [0, \omega]$. Dividing both sides of the above equation by $\tilde{B}(t)$, we have

$$\frac{1}{\tilde{B}} \frac{d\tilde{B}}{dt} = \left(1 - \frac{\tilde{B}(t)}{K(t)}\right) r(t).$$

Integrating both sides of the above equation from 0 to ω, then we have

$$0 = \int_0^\omega \left(1 - \frac{\tilde{B}(t)}{K(t)}\right) r(t)dt,$$

due to the fact that $\tilde{B}(t)$ is ω-periodic.

Hence

$$\lambda_3 = \frac{1}{\omega} \int_0^\omega \left(1 - \frac{2\tilde{B}(t)}{K(t)}\right) r(t)dt < \frac{1}{\omega} \int_0^\omega \left(1 - \frac{\tilde{B}(t)}{K(t)}\right) r(t)dt = 0.$$

Now we have

Theorem 3.9. *In case of* $\max_{t\in[0,\omega]} \tilde{B}(t) \leq c$ *system (5) has a disease-free periodic solution* $(s,\ i,\ B) = (1,\ 0,\ \tilde{B})$*, which is locally asymptotically stable.*

Now we consider the stability of a general positive ω-periodic solution of system (5). We prove the following theorem first.

Theorem 3.10. *Suppose that* $c < \max_{t\in[0,\omega]} \tilde{B}(t)$. *Then there exist an* $\varepsilon > 0$ *and a constant* $T > 0$ *such that, for every solution* $(s(t),\ i(t),\ B(t))$ *of system (5) with positive initial condition, we have*

$$\frac{B(t)}{K(t)} > 1 + \varepsilon, \quad \textit{for} \quad t \geq T. \tag{25}$$

Proof. By the assumption $c < \max_{t\in[0,\omega]} \tilde{B}(t)$ and theorem (3.5), there exist an $\varepsilon_1 > 0$ and a $T_1 > 0$ such that $i(t) \geq \varepsilon_1$ for $t \geq T_1$. Consider equation (5c) and let

$$r(t)B(t)(1 - \frac{B(t)}{K(t)}) + \frac{N\xi i(t)}{2} \geq 0.$$

this inequality hold provided

$$B(t) \leq \frac{K(t) + \sqrt{K^2(t) + \frac{N\xi K(t) i(t)}{r(t)}}}{2}.$$

Hence $\dfrac{dB}{dt} = rB(1 - \dfrac{B}{K}) + N\xi i(t) \geq \dfrac{N\xi\varepsilon_1}{2} > 0$ provided

$$B(t) \leq K(t)\frac{1 + \sqrt{1 + \frac{N\xi\varepsilon_1}{r_M K_M}}}{2}, \quad \text{for} \quad t \geq T_1.$$

It follows

$$\frac{B(t)}{K(t)} \leq \frac{1 + \sqrt{1 + \frac{N\xi\varepsilon_1}{r_M K_M}}}{2} \quad \text{for} \quad t \geq T_1.$$

Taking

$$\varepsilon = \frac{1 + \sqrt{1 + \frac{N\xi\varepsilon_1}{r_M K_M}}}{2} - 1,$$

we see that while $\frac{B(t)}{K(t)} \leq 1 + \varepsilon$, we have $\frac{dB}{dt} \geq \frac{N\xi\varepsilon_1}{2} > 0$. Hence there exists a $T > T_1$ such that

$$\frac{B(t)}{K(t)} > 1 + \varepsilon, \quad \text{for} \quad t \geq T.$$

□

Ecologically, this theorem implies that, as some individuals infected, the bacterial density could surpass the natural carrying capacity, and it may result in more susceptible population get infected even their threshold value c is greater than $\max_{t\in[0,\omega]} \tilde{B}(t)$. It could be a vicious circle if the patients could not be cured in time. And it may cause environmental deterioration in some poor area where medical facilities are insufficient.

Theorem 3.11. *Suppose that* $c < \max_{t\in[0,\omega]} \tilde{B}(t)$. *Then the* ω*-periodic solution* $(s^*(t),\ i^*(t),\ B^*(t))$ *guaranteed by theorem (3.6) is globally asymptotically stable if*

$$a(n+1)\sqrt[n]{\frac{n+1}{n\ln 2}}\exp(-\frac{n+1}{n}) < \frac{r_m\delta H}{2N\xi}. \tag{26}$$

Proof. Let $(s(t),\ i(t),\ B(t))$ be any solution of system (5) with nonnegative initial condition. Define the following Lyapunov function

$$L(t) = |s(t) - s^*(t)| + |i(t) - i^*(t)| + \frac{\delta}{N\xi}|B(t) - B^*(t)|.$$

We calculate the right-hand derivative of $L(t)$ along with system (5) by using the fact that $|x|' = sign(x)x'$:

$$\begin{aligned} D^+L(t) &= sign(s-s^*)(s'-s^{*\prime}) + sign(i-i^*)(i'-i^{*\prime}) + \frac{\delta}{N\xi} sign(B-B^*)(B'-B^{*\prime}) \\ &= sign(s-s^*)\left(\alpha(B^*)s^* - \alpha(B)s - \mu(s-s^*)\right) \\ &+ sign(i-i^*)\left(\alpha(B)s - \alpha(B^*)s^* - \mu(i-i^*) - \delta(i-i^*)\right) \\ &+ \frac{\delta}{N\xi} sign(B-B^*)\left(r(B-B^*) - \frac{r}{K}(B+B^*)(B-B^*) + N\xi(i-i^*)\right). \end{aligned}$$

In any time t, the sign of $i(t)$ and $s(t)$ should be included in the following three cases, and we shall consider three cases respectively.

Case 1 : $sign(s(t) - s^*(t)) = sign(i(t) - i^*(t)) \neq 0.$
Case 2 : $sign(s(t) - s^*(t)) = -sign(i(t) - i^*(t)) \neq 0.$
Case 3 : $sign(s(t) - s^*(t) = 0$ or $sign(i(t) - i^*(t)) = 0.$

Case 1. By theorem (3.10), there exist an $\varepsilon > 0$ and a $T > 0$ such that

$$\begin{aligned} &sign(B(t) - B^*(t))\left(r(t)(B(t) - B^*(t)) - r(t)\frac{B(t) + B^*(t)}{K(t)}(B(t) - B^*(t))\right) \\ &= \left(1 - \frac{B(t)}{K(t)} - \frac{B^*(t)}{K(t)}\right) r(t)|B(t) - B^*(t)| \\ &< -r_m|B(t) - B^*(t)| < 0, \quad \text{for} \quad t > T. \end{aligned}$$

Since

$$\begin{aligned} sign(s-s^*)\left(\alpha(B^*)s^* - \alpha(B)s\right) + sign(i-i^*)\left(\alpha(B)s - \alpha(B^*)s^*\right) = 0, \\ sign(i-i^*)(-\delta(i-i^*)) + \delta sign(B-B^*)(i-i^*) \leq 0, \end{aligned}$$

then

$$D^+L(t) \leq -\mu|s-s^*| - \mu|i-i^*| - r_m\frac{\delta}{N\xi}|B-B^*|, \text{ for } t > T. \tag{27}$$

Case 2. We have four subcases to discuss.

Case 2.1. $s(t) > s^*(t)$ and $B(t) > B^*(t)$.

$sign(s-s^*)\left(\alpha(B^*)s^* - \alpha(B)s\right) + sign(i-i^*)\left(\alpha(B)s - \alpha(B^*)s^*\right) \leq -2\alpha(B)|s-s^*|.$

Thus (27) still holds.

Case 2.2. $s(t) > s^*(t)$ and $B(t) < B^*(t)$.

$$\begin{aligned} &\alpha(B^*)s^* - \alpha(B)s < s\left(\alpha(B^*) - \alpha(B)\right) < \alpha(B^*) - \alpha(B) \\ &= \alpha'(B^* + \theta(B-B^*))(B^*-B) \leq \alpha'_{max}(B^*-B) \quad \text{for some} \quad 0 < \theta < 1, \end{aligned}$$

where α'_{max} denotes the maximum value of $\alpha'(\cdot)$.

Thus

$$D^+L(t) \leq -\mu|s-s^*| - \mu|i-i^*| - \nu\frac{\delta}{N\xi}|B-B^*| \quad \text{for} \quad t > T, \tag{28}$$

where

$$\nu = (r_m - 2\frac{N\xi}{\delta}\alpha'_{max}). \tag{29}$$

It is easy to show that $\alpha'(\cdot)$ reaches its maximum at $\hat{B} = c + H\sqrt[n]{\frac{n}{n+1}\ln 2}$, and

$$\alpha'_{max} \leqslant \alpha'(\hat{B}) = \frac{a(n+1)}{H}\sqrt[n]{\frac{n+1}{n\ln 2}}\exp(-\frac{n+1}{n}).$$

Case 2.3. $s(t) < s^*(t)$ and $B(t) < B^*(t)$.

$$sign(s-s^*)\,(\alpha(B^*)s^* - \alpha(B)s) + sign(i-i^*)\,(\alpha(B)s - \alpha(B^*)s^*) \leq -2\alpha(B^*)|s-s^*|.$$

Case 2.4. $s(t) < s^*(t)$ and $B(t) > B^*(t)$. It is similar to case 2.2.

Now we assume condition (26) holds, then $\nu > 0$. Taking $\zeta = \min\{\mu, r_m,\ \nu\}$, and by (27) and (28), we obtain

$$D^+L(t) \leq -\zeta L(t) \quad \text{for } t > T.$$

Integrating the above inequality over $[T, T']$, we have

$$L(T') - L(T) + \zeta\int_T^{T'} L(t)dt \leq 0.$$

Let $T' \longrightarrow +\infty$ and since $L(\cdot)$ is positive, continuous, and bounded, then $\int_T^{+\infty} L(t)dt$ is finite. By the continuity of $L(t)$, we have

$$\lim_{t\longrightarrow+\infty} L(t) = 0.$$

Namely,

$$\lim_{t\to+\infty}|i(t)-i^*(t)| = 0, \lim_{t\to+\infty}|s(t)-s^*(t)| = 0, \quad \text{and} \quad \lim_{t\to+\infty}|B(t)-B^*(t)| = 0,$$

or

$$\lim_{t\to\infty}(s(t),\ i(t),\ B(t)) = (s^*(t),\ i^*(t),\ B^*(t)). \tag{30}$$

Case 3. Denote $\Delta s = s - s^*$, $\Delta i = i - i^*$, and $\Delta B = B - B^*$. In this case we need to consider two subcases: $\Delta s = 0$ and $\Delta i = 0$. By (5a) and (5b) we have

$$\frac{d(\Delta s + \Delta i)}{dt} = -\mu\Delta s - (\mu+\delta)\Delta i. \tag{31}$$

Case 3.1. $s(t) - s^*(t) = 0$. Under this situation we have

$$\frac{d\Delta i}{dt} = -(\mu+\delta)\Delta i. \tag{32}$$

Thus

$$\Delta i(t) = \Delta i_0\exp(-(\mu+\delta)t). \tag{33}$$

By (5c) we have

$$\frac{d\Delta B}{dt} = r(t)\Delta B - r(t)\frac{B+B^*}{K(t)}\Delta B + N\xi\Delta i.$$

Hence, by lemma (3.10), for $\Delta B > 0$ we have

$$\frac{d\Delta B}{dt} < -r_m\Delta B + \Delta i_0\exp(-(\mu+\delta)) \quad \text{for} \quad t > T, \tag{34}$$

and for $\Delta B < 0$ we have

$$\frac{d\Delta B}{dt} > -r_m\Delta B + \Delta i_0\exp(-(\mu+\delta)) \quad \text{for} \quad t > T, \tag{35}$$

where T is given by lemma (3.10). It is easy to show that equation

$$\frac{dz}{dt} = -r_m z + \Delta i_0\exp(-(\mu+\delta)t) \tag{36}$$

has a globally stable solution $z = 0$. Comparing (34), (35) with (36), by the comparison theorem [23], we have

$$\lim_{t\to\infty} \Delta B = 0.$$

And by (32), obviously we have

$$\lim_{t\to\infty} \Delta i = 0.$$

Thus (30) holds.

Case 3.2. $\Delta i = i(t) - i^*(t) = 0$. By (31) we have

$$\frac{d\Delta s}{dt} = -\mu \Delta s.$$

Thus obviously we have

$$\lim_{t\to\infty} \Delta s(t) = 0.$$

And in this case, by (5c) we have

$$\begin{aligned}\frac{d\Delta B}{dt} &= r(t)\Delta B - r(t)\frac{B+B^*}{K(t)}\Delta B \\ &= r(t)\left(1 - \frac{B+B^*}{K(t)}\right)\Delta B.\end{aligned}$$

Since

$$r(t)\left(1 - \frac{B+B^*}{K(t)}\right) < r(t)(-1-2\varepsilon) < -r_m < 0, \quad \text{for } t > T,$$

we have

$$\lim_{t\to\infty} \Delta B = 0.$$

Thus in this case, (3.11) still holds. □

Now, after the discussion of the above three cases, we have

Corollary 3.12. *Suppose that* $c < \max_{t\in[0,\omega]} \tilde{B}(t)$, *then system (5) admits an unique and globally asymptotically stable* $\omega-$ *periodic solution if*

$$a(n+1)\sqrt[n]{\frac{n+1}{n\ln 2}}\exp(-\frac{n+1}{n}) < \frac{r_m\delta H}{2N\xi}. \tag{37}$$

Remark 3.13. When $\alpha(\cdot)$ takes the form of Holling type described in equation (2), it reaches its maximum at $\hat{B} = c + \sqrt[n]{\frac{n-1}{n+1}}H$,

$$\alpha(\hat{B}) = \frac{a(n+1)\sqrt[n]{(n+1)(n-1)^{n-1}}}{4nH}.$$

the corresponding condition for the global stability of the periodic solution is

$$\frac{a(n+1)\sqrt[n]{(n+1)(n-1)^{n-1}}}{n} < \frac{2r_m\delta H}{N\xi}. \tag{38}$$

Remark 3.14. From the proof of the theorem, it is clear to see that the condition (26) is equivalent to $\max \alpha'(B) < \frac{r_m\delta}{2N\xi}$. Obviously, $\alpha'(B)$ describes the rate that the incidence grows when B increases. If this growth is not so fast; i.e., bounded above by $\frac{r_m\delta}{2N\xi}$, then a unique and globally asymptotically stable periodic solution exists.

Remark 3.15. Taking $c < K$ instead of $c < \max_{t\in[0,\omega]} \tilde{B}(t)$, then corresponding conclusions in this section hold for autonomous system (40).

4. Numerical simulations.

4.1. Simulations for the autonomous system (40).

As space is limited, we omit the case when c is much less than or is much greater than the carrying capacity of bacteria, in which the corresponding system will be stable or be extinct respectively. We only present the reader a special case, in which the system possesses a bistability, when the threshold value c is close to the carrying capacity of bacteria.

Example 4.1. Taking $N = 1 \times 10^6; n = 2; H = 1 \times 10^5; r = 0.25; a = 0.09; \delta = 0.1; \xi = 90; \mu = 1 \times 10^{-4}; c = 10.985 \times 10^6; K = 1 \times 10^6$. Simulation results show that with different initial condition, system may have different local stable states. We found two locally stable states. State I: $X_1 = (s_1, i_1, B_1) = (1.2014 \times 10^{-3}, 9.978 \times 10^{-4}, 1.2805 \times 10^6)$. State II: $X_2 = (s_2, i_2, B_2) = (1_-, 3.7558 \times 10^{-14}, 1_+ \times 10^6)$, here 1_- and 1_+ denote numbers which are very close to 1 but slightly less or greater than 1 respectively. When $B(0)$, the initial value of bacteria, is greater than K, system will approach State I. When $B(0)$ is less than K, system may possibly approach State I or State II, depending on the initial condition $x(0) = (s(0),\ i(0),\ B(0)$. For example given initial condition $x_1(0) = (0.9 \times 10^6, 0.005 \times 10^6, 0.9 \times 10^6)$ and $x_2(0) = (0.9 \times 10^6, 0.00005 \times 10^6, 0.9 \times 10^6)$, system will tend to State I and State II respectively. Note that $x_1(0)$ and $x_2(0)$ have only different initial infective population density. It means that a high level of infective population may cause the environmental deterioration. Over all, with any positive initial condition $x(0)$, corresponding solution will approach one of the two states.

The reader may wonder whether X_2 is essentially $(1,\ 0,\ K)$. Here we emphasize that X_2 is not $(1,\ 0,\ K)$. Firstly, by simulation we see that the final state X_2 is locally independent of initial conditions, which means that X_2 is locally stable. This example is a special case shown in figure 15, where X_1 and X_2 are corresponding to E_3 and E_1, both of which are locally stable. Secondly, the result is in accordance with the computational results given by (41). Thirdly, theoretically system should be permanent according to remark 3.15.

Example 4.2. Take $N = 1 \times 10^6; n = 2; H = 1 \times 10^5; r = 0.25; a = 0.09; \delta = 0.1; \xi = 90; \mu = 1 \times 10^{-4}; K = 1 \times 10^6$, and $c = 1.08 \times 10^6$ is slightly greater than K. Taking $X(0) = (0.1 \times 10^6, 0.000003 \times 10^6, 2 \times 10^6)$, simulation results show that solutions approaches a final state $X = (1.3185 \times 10^{-3},\ 9.9768 \times 10^{-4},\ 1.2805 \times 10^6)$ shown in figure 4.

This example shows that when c is slightly greater than K, with a high density of bacteria in initial condition, solutions may approach a final state $X = (1.3185 \times 10^{-3},\ 9.9768 \times 10^{-4},\ 1.2805 \times 10^6)$ which possesses a bacterial density higher than K. This is also an example to show that $(1,\ 0,\ K)$ is not globally stable in case of $c > K$.

4.2. Simulations for the nonautonomous system.

In what follows, we rewrite the time-dependent bacterial intrinsic growth rate by $\tilde{r}(t)$ and the carrying capacity by $\tilde{K}(t)$ to avoid confusion of notations. To represent seasonal fluctuation, we consider $\tilde{r}(t)$ and $\tilde{K}(t)$ in a simple form as

$$\tilde{r}(t) = r + \frac{r}{4}\sin(\frac{2\pi t}{365}), \tilde{K}(t) = K + \frac{K}{4}\sin(\frac{2\pi t}{365}), \tag{39}$$

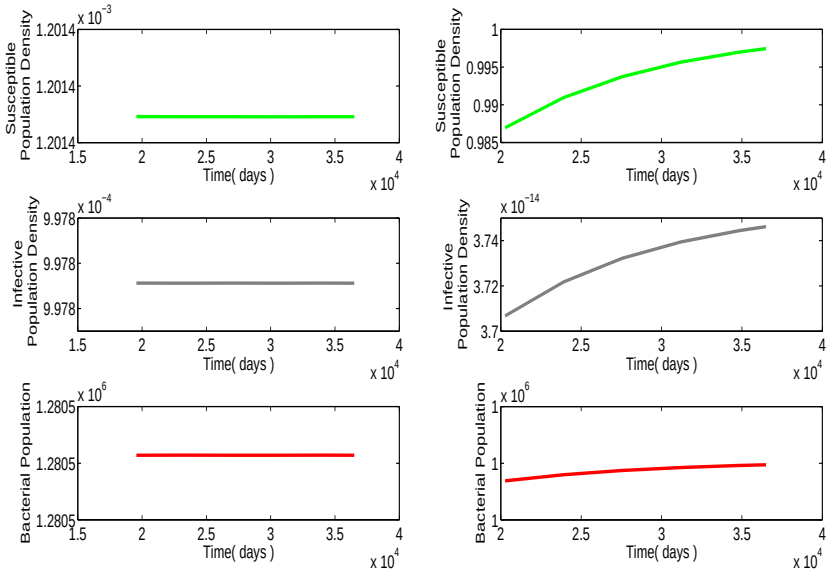

FIGURE 3. System (40) possesses a bistability (See column 1, column 2)

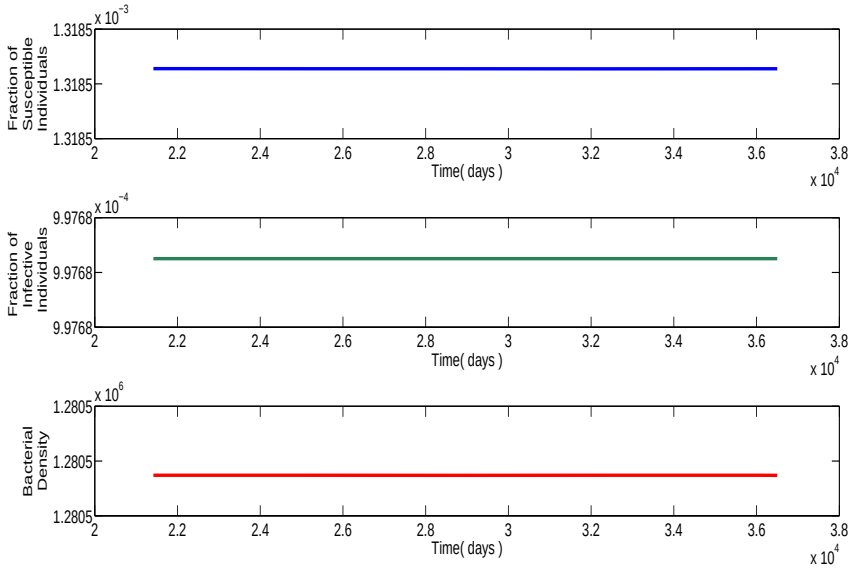

FIGURE 4. An example when system (40) does not approach $(1, 0, K)$ in the case that c is slightly greater than K

with a period $\omega = 365$ days. Here the constants K and r (i.e., the base values of the intrinsic growth rate and carrying capacity) take values listed in Table 1.

Example 4.3. Let us set $n = 1, a = 0.1, \delta = 0.1, r = 10, \xi = 20, \mu = 10^{-4}, c = 10^6, N = 10^6, K = 10^6, H = 10^7$, each of which is in the range of corresponding parameter values listed in table 1. c is significantly less than the peak value of $\tilde{K}(t)$ (1.1×10^6). It's easy to verify that condition (26) is satisfied. Simulation results are shown in figure 5. We clearly observe a stable periodic solution. In particular, the peak values of the susceptible and infective individuals occur periodically at times when the bacterial concentration is rapidly ascending. See figure 5.

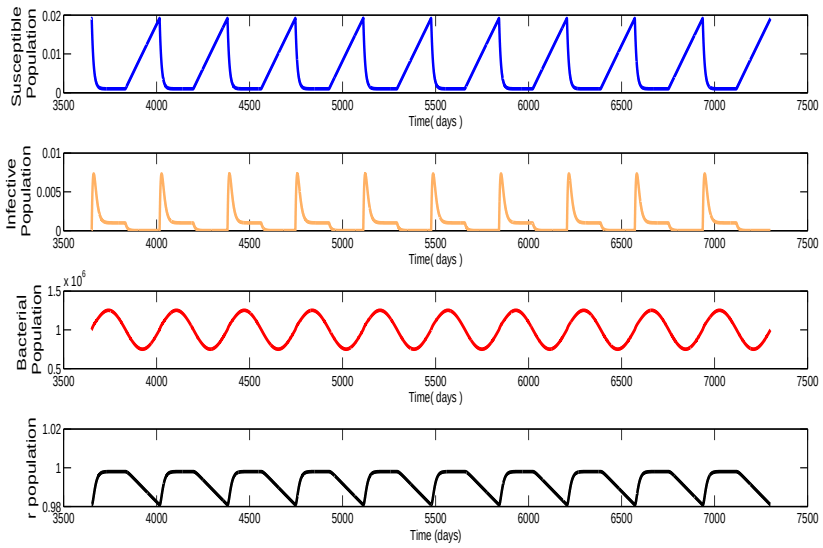

FIGURE 5. Populations of system (5) approach a periodic solution

Example 4.4. When the threshold of immunity is significantly higher then the maximum of carrying capacity of bacteria, solutions of system (5) might tend to a disease free periodic solution $(1, 0, \tilde{B})$. See figure 6, where we take $n = 1, a = 0.1, \delta = 0.1, r = 10, \xi = 20, \mu = 10^{-4}, c = 1.5 \times 10^6, N = 10^6, K = 10^6, H = 10^7$.

Example 4.5. When c is close to maximum of $K(t)$, slightly less than maximum of $\tilde{B}(t)$, H is relatively low, ξ is relatively high, such as $K = 1 \times 10^6, N = 1 \times 10^6, r = 0.25, \delta = 0.1, \xi = 90, \mu = 1 \times 10^{-4}, H = 5 \times 10^5, a = 0.1, n = 2$, and seasonal fluctuation is mild, say $r(t) = (1 + 1/10 * sin(t))r$; $K(t) = (1 + 1/10 * sin(t))K$, system (5) may have different locally stable state, depending on initial conditions. It's easy to verify that condition (26) is not satisfied. Presently we have detected three kind of different final states. Taking the initial values $x_0(0) = (0.2 \times 10^6, 0.00001 \times 10^6, 1.2 \times 10^6)$(Here $B(0)$ is higher than the peak value of $K(t)$), system will approach to a stable state $\tilde{X} = (s_0(t), i_0(t), B_0(t))$, which is a periodic solution fluctuating around $(9.99 \times 10^{-4}, 9.98 \times 10^{-4}, 1.27 \times 10^6)$, (See figure 7, right column). Taking $x_1(0) = (0.2 \times 10^6, 0.00001 \times 10^6, 0.8 \times 10^6)$ (Here $B(0)$ is less than the peak value of $K(t)$) system will tend to the second kind of final state $X_1(t)$, which is mainly very close to the disease free solution $(0, 0, \tilde{B}(t))$, and occasionally accompanied by short time eruptions of infection(See figure7, left

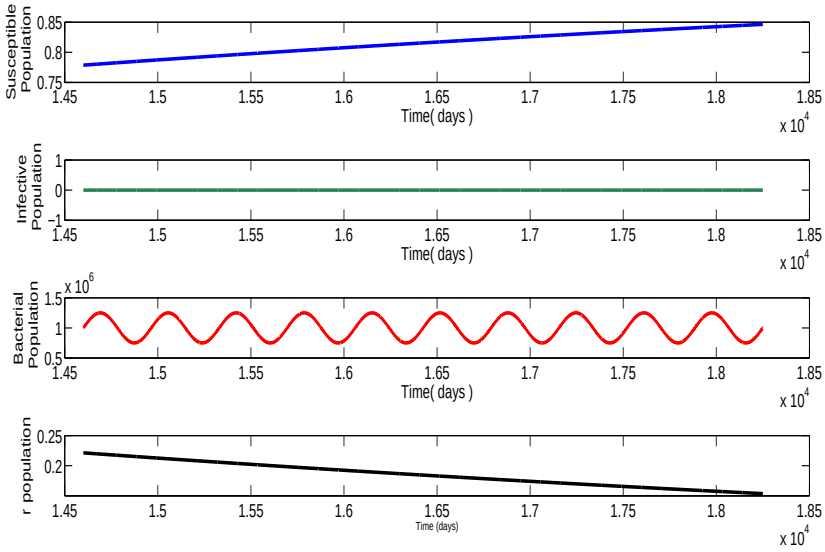

FIGURE 6. When the threshold of immunity is significantly higher than the maximum of bacterial capacity, populations of system (5) tend to a disease free periodic solution

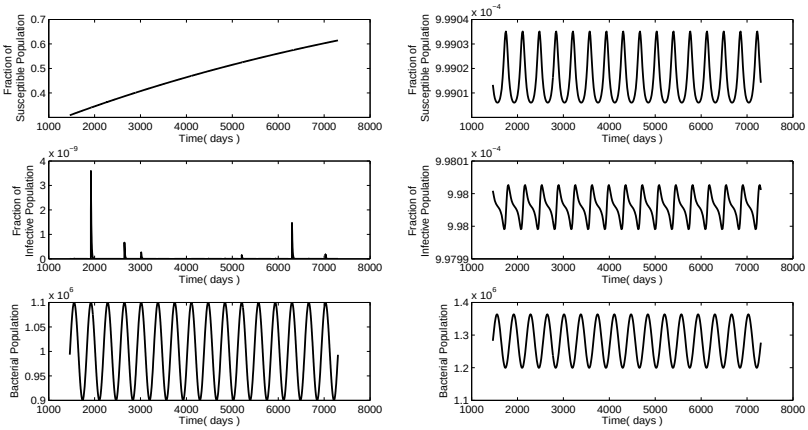

FIGURE 7. Two final states of system (5) depending on different initial values

column). Taking $x_2(0) = (0.2\times10^6, 0.01\times10^6, 0.8\times10^6)$ system will approach to the third kind of final state $X_2(t)$. Noticing that while initial conditions $x_1(0)$ and $x_2(0)$ has the same fraction of susceptible population and bacterial density, $X_2(0)$ has a higher fraction of infective population. After having experienced a large scale of outbreak of infection, $X_2(0)$ leads the system to a different final state $X_2(t)$, which has a higher bacterial density and a sharp declining of the fraction of susceptible population than $X_1(t)$. Obviously $X_2(t)$ marks a worsen environment(due to the higher bacterial density). In the simulation from the enlarged figure of infective population, we can detect a lot of short time eruptions with different scales. These

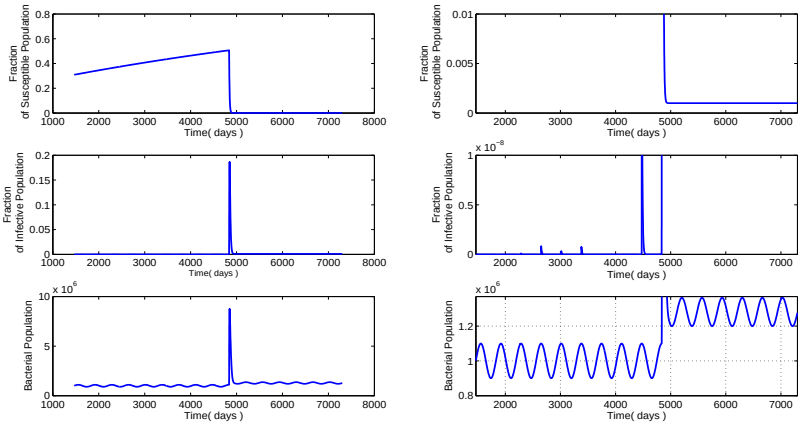

FIGURE 8. The third final state of system (5) and the locally enlarged figure (shown in the right column)

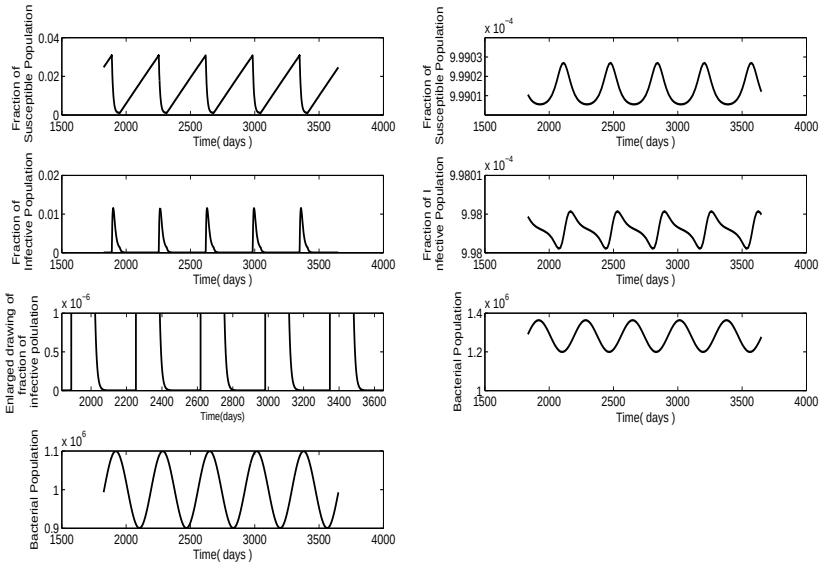

FIGURE 9. Periodic outbreak of epidemic ($\xi = 0$, left column), and durative infection ($\xi = 90$, right column)

eruptions are caused by the fluctuation of bacterial density. When the peak of bacterial density comes, it surpasses the threshold value of susceptible population, with a proper initial condition, it could result in a swift infection. But the scale of eruption may depend on how long and how much the peak values of bacterial density surpass the threshold value. Some times, the scale could be very large(See the left column of figure (8), nearly 20 percent of population are infected in the coming of the peak of bacteria fluctuation), and has a long term influence on the system, and results in a high bacterial density environment. Sometimes the scale

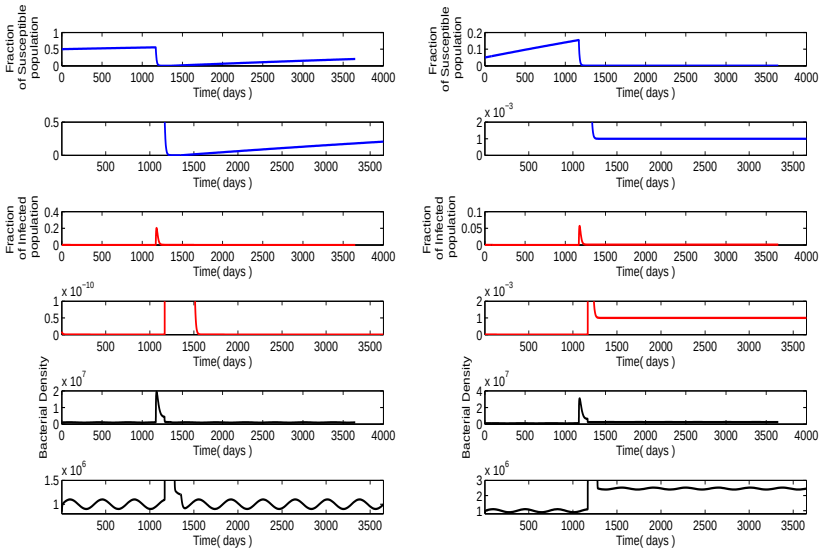

FIGURE 10. System encounters a sudden event. Left column: $N = 1 \times 10^6$. Right column: $N = 1 \times 10^7$.

could be very small, say lower than 10^{-10}(See the left column of figure 7), and it could hardly be detected. In reality this might not represent an infected individual, but still it could be treated as a very slight infection of individuals. Practically when a person is infected in such a slight degree, he may be uninfected.

Example 4.6. In this example we consider two different situations when xi is zero or nonzero. Taking $c = 1.085 \times 10^5$, which is slightly less than the peak value of $\tilde{B}(t)$, the bacterial density in disease free system, and values of other parameters are as in Example 4.5. Taking initial value $x(0) = (7.5 \times 10^6, 0.05 \times 10^6, 1 \times 10^6)$. We see that when $\xi = 0$, there is an outbreak of epidemic every year which is synchronous with the peak value of $\tilde{B}(t)$, and after this short period, the fraction of infective population is very low(nearly zero), and the average fraction of susceptible population is between 1 percent and 2 percent, namely there are about 1 to 2 percent of people remain uninfected. When $\xi = 90$, the fractions of susceptible and infective population are both nearly 0.001, and this shows that there are only 0.1 percent of the total population are not infected. Strictly speaking, they are totally two different models when $\xi = 0$ and $\xi > 0$. These two models are fit for different environment. In those places, when population density is low, and public sanitation is relatively good, and people have less contact, the model for $\xi = 0$ is suitable. In places when population density is high, public sanitation is bad, and people may have to contact frequently, the model for $\xi > 0$ is more suitable. In short, when $\xi > 0$, infection between people are considered. See figure 9.

Example 4.7. In this example we assume the biological system encounters a sudden event, say an abnormal reproduction of bacteria due to the major natural disasters. Take $K = 1 \times 10^6$, $r = 0.25$, $\delta = 0.1$, $\xi = 90$, $\mu = 1 \times 10^{-4}$, $H = 8 \times 10^5$, $a = 0.1$, $n = 2$, $x(0) = (0.5 \times 10^6, 0.001 \times 10^6, 0.8 \times 10^6)$. For $c = 1.2 \times 10^6$, which is significantly higher than the peak value of $K(t)$, normally system will tend to a

disease free state. However, when system encounters a sudden event, it may have a different behavior depending on system parameters. These simulations are in connection with total populations. In the first case, taking $N = 1 \times 10^6$, system experienced a severe infection, caused a sharp declining of the fraction of susceptible population. After that, the state of the system gradually recovers to the primary state (See the left column of the figure 10). In the second case, taking $N = 1 \times 10^7$, we find that the sudden event brings a long term influence on the system behavior. After a severe infection, system tend to a new stable state. The fraction of susceptible population has a vast slash, and the fraction of infection population has a substantial increase, and the bacterial density rises to a higher level (See the right column of figure 10). This new state marks a worsen environment caused by the sudden event.

Remark 4.8. From these examples, we observe that the threshold value c is critical in determining the dynamical behaviors. In section 3, we have obtained a sufficient condition for the stability of system (5) when c is less than the peak value of $\tilde{B}$. However when c is significantly less than the peak value of $\tilde{B}$, the condition is not important for the stability. This can be explained as follow. From the process of the above proof, we see that when $c < \max_{t\in[0,\omega]} \tilde{B}(t)$the condition for the stability of the periodic solution suffices to $\nu > 0$. When c is much less then $\max_{t\in[0,\omega]} \tilde{B}(t)$ or the carrying capacity of bacteria, $\alpha(B)$ could be much greater than 0, which implies a greater A in (10), and a greater ε_2 in (18), which in turn implies a greater i by (8). Thus by the proof of lemma (3.10), it implies a greater B. When B is much greater then $\hat{B}$, $\alpha'(B)$ could be much less than $\alpha'(\hat{B})$, and thus condition $\nu > 0$ could be much easier to be satisfied, which means the stability of the periodic solution. When c is close to $\max_{t\in[0,\omega]} \tilde{B}(t)$ or the carrying capacity of bacteria, condition (26) is crucial to determine whether the periodic solution is stable or not.

Comparatively, the nonautonomous model is more realistic than the autonomous one. As it is shown in Example 4.1, 4.3-4.7, nonautonomous model exhibits more complexities especially when c is close to the peak value of $K(t)$. Example 4.6 presents an interesting phenomena that an eruption of epidemic may occur unexpectedly. This is congruent to what we encounter in reality.

5. **Discussion.** Cholera remains epidemic and endemic regionally in the world, especially in the locations lacking adequate sanitation and water infrastructure. With the continuing outbreaks, mathematical modeling plays an important role in deciphering its dynamics and providing suggestions for governments and health organizations to take effective actions. Cholera is an indirectly transmitted infectious disease, and recent modeling efforts have been made in this direction, such as the addition of an environmental pool and the incorporation of an immunological threshold for infection [4, 10, 11]. Subject to the annual variation of temperature, nutrients, rainfall, etc. in the reservoir, seasonality is believed to be pivotal in determining cholera epidemics and endemism [6, 17]. Seasonal drivers have been recently incorporated in cholera transmission models [5, 15, 16]. In this paper, we incorporate the seasonal factor explicitly in bacterial growth term and discuss its impact on cholera dynamics. In addition, we originally introduce a new threshold incidence function which is infinitely smooth. Our proposed incidence function biologically mimics the standard Holling type functions, and the smoothness of the new incidence form allows us to perform rigorous and deeper mathematical analysis for the complicated dynamics of an indirectly transmitted infectious disease.

It is mathematically challenging to analyze a high-dimensional nonautonomous system. In the paper, we provide the forward invariance, the uniform persistence, the existence of periodic solutions, and their stability (local and global), for our nonautonomous model. Forward invariance and persistence illustrate the rationality of the proposed seasonal forcing model. The immunological threshold is the key parameter in determining persistence, periodic solutions and their stability, that is, the mean infection threshold of susceptible individuals in an epidemic region is critical in determining cholera outbreaks and their severity. Hence in order to prevent an outbreak of cholera, we have either to raise the immunity of susceptible individuals or to improve the local environments, bring down the carrying capacity of bacteria which determines the periodic solution $\tilde{B}$ in our model. To prove the persistence and the stability of periodic solutions for a nonautonomous high-dimensional dynamical system is of considerable challenge. Our proofs are new and may be applicable to other models of this type. Our numerical simulations validate our mathematical results.

Further steps to take with the seasonal forcing model would be to refine the conditions on the global stability results of periodic solutions. The imposed conditions are sufficient but not necessary for global stability. To verify and calibrate the nonautonomous model with seasonality, we should fit our theoretical outputs to empirical data from regional cholera outbreaks such as the reported cases in Bangladesh and Haiti. The seasonality is clearly required to fit a multi-year data set. In the modeling perspective, it is important to mechanistically incorporate temperature, nutrients, and sudden events such as hurricane and eddy flow, for the environmental reservoir.

Acknowledgments. We would like to thank the MBI (Mathematical Biosciences Institute) at the Ohio State University for providing a platform for the communication and collaboration of the authors.

Appendix A. **Equilibria of the autonomous system.** We start our analysis by examining the equilibria of the autonomous model. Since $S + I + R = N$ where the total population N is a constant, we will drop R from the system. Meanwhile, introducing $s = S/N, i = I/N$, we obtain an equivalent form to the system (1):

$$\begin{cases} \dfrac{ds}{dt} = & -\alpha(B)s - \mu s + \mu \,, & \text{(40a)} \\ \dfrac{di}{dt} = & \alpha(B)s - \mu i - \delta i \,, & \text{(40b)} \\ \dfrac{dB}{dt} = & rB(1 - \frac{B}{K}) + N\xi i \,, & \text{(40c)} \end{cases}$$

where the saturation function $\alpha(B)$ takes the exponential form of (3).

An equilibrium (s^*, i^*, B^*) of system (40) satisfies

$$\begin{cases} s^* & = \dfrac{\mu}{\mu + \alpha(B^*)}, & \text{(41a)} \\ i^* & = \dfrac{\mu}{\mu + \delta} \dfrac{\alpha(B^*)}{\mu + \alpha(B^*)} \,, & \text{(41b)} \\ rB^*(\dfrac{B^*}{K} - 1) & = N\xi i^*. & \text{(41c)} \end{cases}$$

System (40) has possibly two, three or four equilibria. The exact number of equilibrium points not only depends on the threshold value c, but also on the values of parameters of $K, r, N, \xi, \mu, \delta$, etc. However, in any case $E_0(1,0,0)$ is an equilibrium of system (40). Combining (41b) and (41c) we form an equation

$$B(B-K) = \nu \frac{\alpha(B)}{\mu + \alpha(B)}, \tag{42}$$

where $\nu = \dfrac{NK\xi\mu}{r(\mu+\delta)}$.

Denote

$$f(B) \triangleq B(B-K), \qquad g(B) \triangleq \nu \frac{\alpha(B)}{\mu+\alpha(B)}. \tag{43}$$

Thus equation (42) is equivalent to

$$f(B) = g(B).$$

Now we will work out the number of equilibrium points of equation (42) through the functions $f(B)$ and $g(B)$. Though $f(B)$ is quite simple, we still need some analysis to get a few characteristics of $g(B)$.

Denote $h_n(B) = \frac{nH^n \ln 2}{(B-c)^n}$. By (3), we have

$$\alpha'(B) = \begin{cases} 0, & B \le c, \\ \frac{h_n}{(B-c)}\alpha(B), & B > c, \end{cases} \tag{44}$$

$$g'(B) = \begin{cases} 0, & B \le c, \\ \frac{\mu\nu h_n}{(B-c)} \frac{\alpha(B)}{(\mu+\alpha(B))^2}, & B > c, \end{cases} \tag{45}$$

$$g''(B) = \begin{cases} 0, & B \le c, \\ \frac{\mu\nu h_n}{(B-c)^2} \frac{\alpha(B)}{(\mu+\alpha(B))^2} \left(-(n+1) + \frac{\mu-\alpha(B)}{\mu+\alpha(B)} h_n\right), & B > c. \end{cases} \tag{46}$$

Now we can easily show (proof omitted) that the function $g(B)$ satisfies

(i): $g(B) = 0$, as $B \le c$.
(ii): $g(B)$ is strictly increasing as $B > c$.
(iii): $g(B)$ has an unique inflection point $\bar{B}$ given by

$$\frac{(B-c)^n(n+1)}{H^n n \ln 2} = \frac{\mu - \alpha(B)}{\mu + \alpha(B)}. \tag{47}$$

(iv): $g(B)$ is convex in $[0,\bar{B}]$, and is concave in $[\bar{B}, \infty)$.
(v): $g(B)$ is infinitely smooth.

The third property of $g(B)$ is a direct result of the following proposition.

Proposition A.1. *Equation (47) possesses a unique root $\bar{B}$.*

Proof. Let $u(B) = \frac{(B-c)^n(n+1)}{H^n \ln 2}$; $v(B) = \frac{\mu-\alpha(B)}{\mu+\alpha(B)}$. Obviously $u(c) = 0$, and $u(B)$ is increasing in $[c, \infty)$ satisfying $u(\infty) = +\infty$; $v(c) = 1$, and $v(B)$ is decreasing in $[c, \infty)$ satisfying $v(\infty) < 0$. Let $w(B) = v(B) - u(B)$, then we have $w(c) = 1 > 0$. Let $B^0 = \alpha^{-1}(\mu) > c$, then $u(B^0) > 0$ and $v(B^0) = 0$, hence $w(B^0) < 0$. Since $w(\cdot)$ is continuous, by the intermediate value theorem, there exist a point $\bar{B}$ such that $w(\bar{B}) = 0$. By the monotonicity of $w(\cdot)$, the root of equation (47) is unique. □

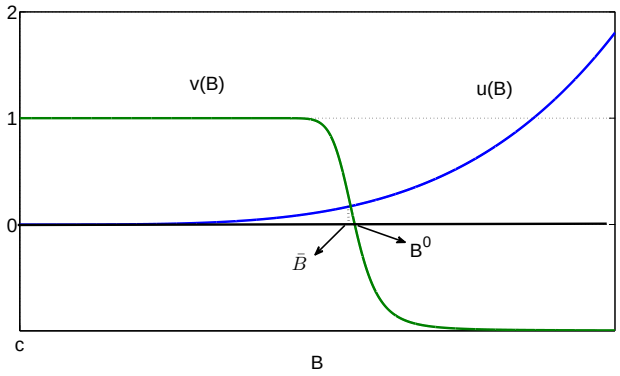

FIGURE 11. Curves of $u(B)$ and $v(B)$ have an unique intersection $\bar{B}$

From the discussion above we can see that the shape of the curve of function $g(B)$ is quite similar to that of $\alpha(B)$. What is important is that the shape is directly related to the number of equilibria of the system.

Let $g_c(B) = g(B+c)$. Given a number M_x that is large enough, when c increases from 0 to M_x, the curve $g_c(B)$ has a parallel translation from passing the origin, to crossing the curve $f(B)$, and then to the positive direction of B axis. The influence of the threshold value c on the equilibria of system (40) can be seen in this process of movement.

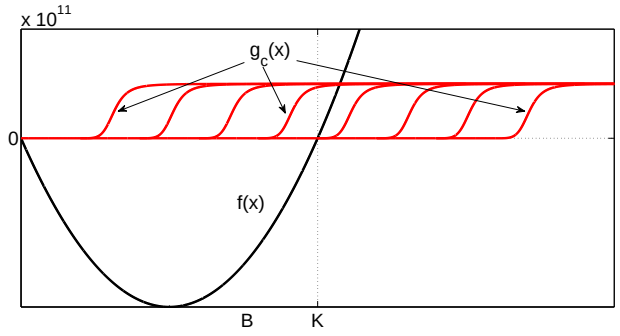

FIGURE 12. Curves of function f and g with changing threshold values c.

By the properties of function g we can see that it is at $\bar{B}$ that the function $g'(B)$ reaches its maximum. It means that at $\bar{B}$ the curve of $g(B)$ reaches its maximal slope. By (iii) we have a preliminary estimate of $\bar{B}$.

$v(B) = 0$ has a root $B^0 = c + \frac{H}{\sqrt[n]{\log_2^{\frac{a}{\mu}}}}$, and we have $\bar{B} \in (c,\ B^0)$. On the other hand, if we take $B_- = c + \frac{H}{\sqrt[n]{1+\log_2^{\frac{a}{\mu}}}}$, we have $\alpha(B_-) = \frac{\mu}{2}$ and $g''(B_-) > 0$ provided values of parameters are taken in Table 1 and it means $B_- < \bar{B}$. Hence we have

$\bar{B} \in (B_-, B^0)$.

$$\frac{H}{\sqrt[n]{1+\log_2^{\frac{a}{\mu}}}} < \bar{B} - c < \frac{H}{\sqrt[n]{\log_2^{\frac{a}{\mu}}}}.$$

Denote the point corresponding to $\bar{B}$ in the curve of function $g(B)$ as M. If the position of M corresponding to $c = 0$ is on the left of the curve of function $g(B)$, then as c increases from 0 to large enough, M has a parallel movement from left to right along the positive B axis and it will pass through $g(B)$. There must be a point c such that M is on the curve of function $f(B)$, and we denote the corresponding abscissa as $\bar{B}_M$. At $\bar{B}_M$ we possibly have

Case i). $g'(\bar{B}_M) \le f'(\bar{B}_M)$, and

Case ii). $g'(\bar{B}_M) > f'(\bar{B}_M)$.

Both cases are possible depending on the parameter values we choose.

In fact, on one hand,

$$g'_{max}(B) = g'(\bar{B}_M) > g'(B^0) = \frac{n\mu\nu \ln 2}{(B^0 - c)} \frac{H^n}{(B^0 - c)^n} \frac{\alpha(B^0)}{(\mu + \alpha(B^0))^2}$$

$$= \frac{n\nu}{4H} \log(\frac{a}{\mu}) \sqrt[n]{\log_2 \frac{a}{\mu}} \triangleq g_1,$$

$$f'(\bar{B}_M) < f'(B^0) = 2B^0 - K \triangleq f_2,$$

On the other hand,

$$g'(\bar{B}_M) = \frac{\nu h_n}{(\bar{B}_M - c)} \frac{\mu}{\alpha(\bar{B}_M)} \left(\frac{\alpha(\bar{B}_M)}{\mu + \alpha(\bar{B}_M)} \right)^2 < \frac{\nu h_n}{(\bar{B}_M - c)} \frac{\mu}{\alpha(\bar{B}_M)}$$

$$= \frac{n\nu\mu H^n \ln 2}{(\bar{B}_M - c)^{n+1}} \frac{1}{\alpha(\bar{B}_M)} \le \frac{n\nu\mu H^n \ln 2}{(B_- - c)^{n+1}} \frac{1}{\alpha(B_-)} = \frac{2n\nu}{H} \ln(\frac{2a}{\mu}) \sqrt[n]{\log_2^{\frac{2a}{\mu}}} \triangleq g_2,$$

$$f'(\bar{B}_M) = 2\bar{B}_M - K > 2B_- - K \triangleq f_1.$$

Hence we have

$$f'(\bar{B}_M) \in (f_1, f_2), \quad g'(\bar{B}_M) \in (g_1, g_2). \tag{48}$$

For illustration, let us pick the parameter values $N = 10^6, n = 2, r = 0.3, K = 10^6, H = 10^6, a = 0.1, \delta = 0.1, \xi = 90, \mu = 9 \times 10^{-5}, c = 10^6$, all within biologically meaningful ranges (see Table 1). we have

$$f'(\bar{B}_M) \in (1.600 \times 10^6, 1.629 \times 10^6), \quad g'(\bar{B}_M) \in (3.009 \times 10^6, 27.726 \times 10^6),$$

thus we obtain

$$g'(\bar{B}_M) > f'(\bar{B}_M).$$

If we change the value of H, the half saturation density, from 10^6 to 10^7 and keep the values of other parameters unchanged, then we have

$$f'(\bar{B}_M) \in (6.9982 \times 10^6, 7.2876 \times 10^6), \quad g'(\bar{B}_M) \in (0.3009 \times 10^6, 2.7726 \times 10^6),$$

and

$$g'(\bar{B}_M) < f'(\bar{B}_M).$$

When the value of the parameter H varies, the system(5) has possibly two, three or four equilibria (including E_0).

Proposition A.2. *Let $\bar{B}$ be the solution of equation(47), if $g'(\bar{B}) \le K$, then system (40) possesses two equilibria: $E_0(1, 0, 0)$ and $E_1(s^*, i^*, B^*)$.*

Proof. we only need to prove that apart from E_0, Equation (42) has only one equilibrium E_1.

In fact, for $0 < B \leq K$, $f(B) \leq 0$ and $g(B) > 0$, equation $f(B) = g(B)$ will have no root apart from E_0 in $[0, K]$. For $B > K$, $f'(B) = 2 * B - K > K$, while $g'(B) \leq g'(\bar{B}) \leq K$. Let $U(t) = f(t) - g(t)$, then obviously we have $U(K) < 0$, $U(+\infty) > 0$ and $U(t)$ is monotone in $[K, +\infty)$(This is implied by the truth that $f'(B) - g'(B) > 0$ for $B > K$). Hence $U(t)$ has an unique zero point in $[K, +\infty)$, namely equation (42) has an unique equilibrium in $[K, +\infty)$. □

For $g'(\bar{B}) > K$, system (40) has possibly two, three, and four equilibria. For example, taking $N = 10^6, r = 0.27, K = 10^6, \delta = 0.1, \xi = 90, \mu = 10^{-4}, H = 10^6, a = 0.09$, and gradually increasing the value of c from approximately 6.94×10^5 to 9.17×10^5, we obtain different numbers of equilibria (See Figures 13-15).

Appendix B. **Stability of the autonomous system.** We now analyze the stability of the equilibria for the autonomous model. The Jacobian of system (40) is

$$J = \begin{pmatrix} -\alpha(B) - \mu & 0 & -\alpha'(B)s \\ \alpha(B) & -\mu - \delta & \alpha'(B)s \\ 0 & N\xi & r(1 - \frac{2B}{K}) \end{pmatrix}. \tag{49}$$

In particular, the Jacobian corresponding to $E_0(1, 0, 0)$ is

$$J_0 = \begin{pmatrix} -\mu & 0 & 0 \\ 0 & -\mu - \delta & 0 \\ 0 & N\xi & r \end{pmatrix}. \tag{50}$$

Since J_0 has three eigenvalues, $-\mu$, $-\mu - \delta$ and r, two of which are negative and the third one is positive, we have

Theorem B.1. *The disease-free equilibrium $E_0(1, 0, 0)$ for system (40) is an unstable saddle-node.*

In case of $c > K$, system (40) possesses another equilibrium $E_1(1, 0, K)$, and the corresponding Jacobian is

$$J_1 = \begin{pmatrix} -\mu & 0 & 0 \\ 0 & -\mu - \delta & 0 \\ 0 & N\xi & -r \end{pmatrix}. \tag{51}$$

The characteristic polynomial of J_1 is

$$Det(\lambda I - J_1) = \begin{vmatrix} \lambda + \mu & 0 & 0 \\ 0 & \lambda + \mu + \delta & 0 \\ 0 & -N\xi & \lambda + r \end{vmatrix}$$
$$= (\lambda + \mu)(\lambda + \mu + \delta)(\lambda + r)$$

Since all eigenvalues of J_1 are negative, we have

Theorem B.2. *In case of $c > K$, system (40) possesses an equilibrium $E_1(1, 0, K)$, which is locally asymptotically stable.*

For any other equilibrium $E(s^*, i^*, B^*)$ besides $E_0(1, 0, 0)$ and $E_1(1, 0, K)$, we consider the characteristic polynomial of E,

$$Det(\lambda I - J) = \begin{vmatrix} \lambda + \alpha(B^*) + \mu & 0 & \alpha'(B^*)s^* \\ -\alpha(B^*) & \lambda + \mu + \delta & -\alpha'(B^*)s^* \\ 0 & -N\xi & \lambda + r(\frac{2B^*}{K} - 1) \end{vmatrix}$$

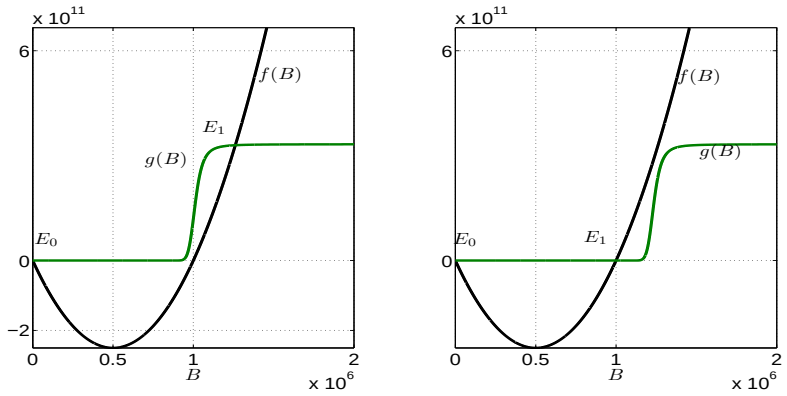

FIGURE 13. System (40) has two equilibria

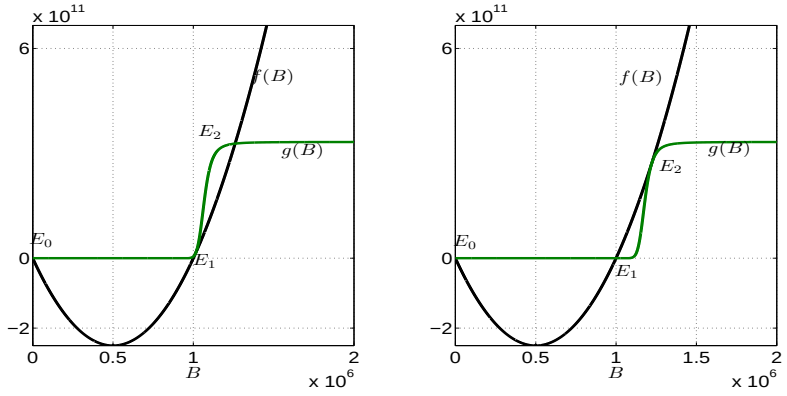

FIGURE 14. System (40) has three equilibria

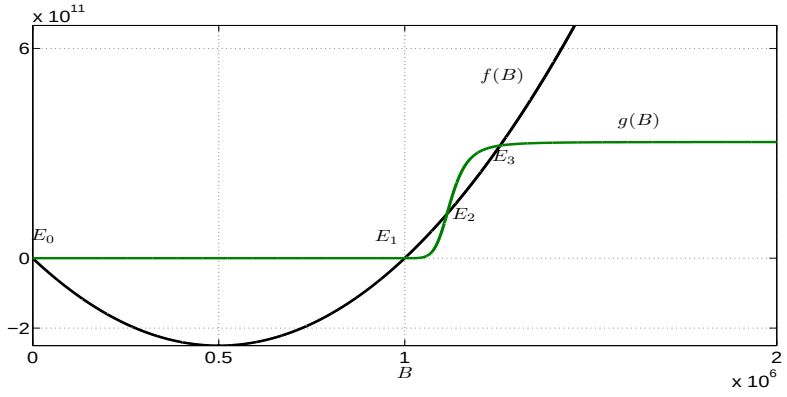

FIGURE 15. System (40) has four equilibria

$$= a_0\lambda^3 + a_1\lambda^2 + a_2\lambda + a_3, \tag{52}$$

where

$a_0 = 1$,
$a_1 = \alpha(B^*) + 2\mu + \delta + r(\frac{2B^*}{K} - 1)$,
$a_2 = (\alpha(B^*) + \mu)(\mu + \delta) + r(\frac{2B^*}{K} - 1)(\alpha(B^*) + \mu) + r(\frac{2B^*}{K} - 1)(\mu + \delta) - N\xi\alpha'(B^*)s^*$,
$a_3 = r\left(\frac{2B^*}{K} - 1\right)(\alpha(B^*) + \mu)(\mu + \delta) - \mu N\xi\alpha'(B^*)s^*$.

To proceed, we apply the following standard result from the Routh-Hurwitz stability criterion:

Lemma B.3. *The necessary and sufficient condition for the polynomial (52) to be stable is*

$$a_0 > 0,\ a_1 > 0,\ a_2 > 0,\ a_3 > 0 \quad \textit{and} \quad a_1a_2 > a_0a_3.$$

The condition $a_0 > 0$ is trivial. Since $B^* > K$, we obtain $a_1 > 0$.

According to (42), we have

$$B^*(B^* - K) < \nu.$$

Hence,

$$K < B^* < \frac{K}{2}\left(1 + \sqrt{1 + \frac{4\nu}{K^2}}\right), \tag{53}$$

and we have

$$2 < \frac{2B^*}{K} < 1 + \sqrt{1 + \frac{4\nu}{K^2}}. \tag{54}$$

Denote

$$F(B) = rB(1 - \frac{B}{K}) + N\xi i(B).$$

Obviously

$$F(B) = \frac{r}{K}(-f(B) + g(B)), \tag{55}$$

$$F'(B^*) = r(1 - \frac{2B^*}{K}) + N\xi\frac{\mu}{\mu + \delta}\frac{\mu}{(\mu + \alpha(B^*))^2}\alpha'(B^*)$$

$$= -r(\frac{2B^*}{K} - 1) + N\xi\frac{\mu}{(\mu + \delta)(\mu + \alpha(B^*))}\alpha'(B^*)s^*$$

$$= -\frac{1}{(\mu + \delta)(\mu + \alpha(B^*))}a_3.$$

If $a_3 \le 0$, according to Lemma (B.3), the corresponding equilibrium is unstable. The condition $a_3 \le 0$ is equivalent to $F'(B^*) \ge 0$, and also equivalent to $f'(B^*) \le g'(B^*)$, which means the slope of the curve of $g(B^*)$ is equal or steeper than that of $f(B^*)$. This result provides an intuitive way for the judgment of the instability of the equilibrium $E(s^*, i^*, B^*)$, which we refer to as a geometrical method. We state the above results as follow.

Theorem B.4. *Suppose*

$$F(B) = rB(1 - \frac{B}{K}) + N\xi i(B),$$

where $i(B)$ is defined as in equation (41b). Then equilibrium $E(s^*, i^*, B^*)$ of system (40) is unstable if $F'(B^*) \ge 0$.

An equivalent statement is

Theorem B.5. *Suppose $f(B)$ and $g(B)$ are defined by (43), then equilibrium $E(s^*, i^*, B^*)$ is unstable if $f'(B^*) \le g'(B^*)$, geometrically the slope of the tangent line of $f(B)$ equals or is less than that of $g(B)$ at B^*.*

Now we will seek a sufficient condition for the local stability of a general equilibrium apart from $E_0(1,0,0)$ and $E_1(1,0,K)$. Suppose

$$r(\frac{2B^*}{K} - 1)(\mu + \delta) > N\xi\alpha'(B^*)s^* \tag{56}$$

holds, then

$$\begin{aligned} a_3 &= r(\frac{2B^*}{K} - 1)\alpha(B^*)(\mu+\delta) + \mu\left(r(\frac{2B^*}{K} - 1)(\mu+\delta) - N\xi\alpha'(B^*)s^*\right) \\ &> r(\frac{2B^*}{K} - 1)\alpha(B^*)(\mu+\delta) > 0, \\ a_2 &= (\alpha(B^*)+\mu)(\mu+\delta) + r(\frac{2B^*}{K} - 1)(\alpha(B^*)+\mu) + r(\frac{2B^*}{K} - 1)(\mu+\delta) - N\xi\alpha'(B^*)s \\ &> (\alpha(B^*)+\mu)(\mu+\delta) + r(\frac{2B^*}{K} - 1)(\alpha(B^*)+\mu) > 0, \text{ and} \\ a_1a_2 &> r\left(\frac{2B^*}{K} - 1\right)(\alpha(B^*)+\mu)(\mu+\delta) > a_0a_3. \end{aligned}$$

Hence, according to Lemma (B.3), condition (56) is a sufficient condition for the stability of nontrivial equilibrium $E(s^*, i^*, B^*)$. It is easy to show that condition (56) is equivalent to

$$f'(B^*) > \left(1 + \frac{\alpha(B^*)}{\mu}\right) g'(B^*). \tag{57}$$

Hence we have

Theorem B.6. *Equilibrium $E(s^*, i^*, B^*)$ is stable if condition (57) holds.*

Geometrically, this theorem suggests that if the slope of the tangent line of $f(B)$ at B^* is much larger than that of $g(B)$, then the equilibrium $E(s^*, i^*, B^*)$ is locally asymptotically stable.

REFERENCES

[1] J. R. Andrews and S. Basu, Transmission dynamics and control of cholera in Haiti: An epidemic model, *Lancet*, **377** (2011), 1248–1255.

[2] E. Bertuzzo, L. Mari, L. Righetto, M. Gatto, R. Casagrandi, M. Blokesch, I. Rodriguez-Iturbe and A. Rinaldo, Prediction of the spatial evolution and effects of control measures for the unfolding Haiti cholera outbreak, *Geophys. Res. Lett.*, **38** (2011), L06403.

[3] D. L. Chao, M. E. Halloran and I. M. Longini, Vaccination strategies for epidemic cholera in Haiti with implications for the developing world, *Proc. Natl. Acad. Sci.*, **108** (2011), 7081–7085.

[4] C. T. Codeço, Endemic and epidemic dynamics of cholera: The role of the aquatic reservoir, *BMC Infect. Dis.,* **1** (2001), p1.

[5] M. C. Eisenberga, G. Kujbidad, A. R. Tuited, D. N. Fismand and J. H. Tiena, Examining rainfall and cholera dynamics in Haiti using statistical and dynamic modeling approaches, *Epidemics,* **5** (2013), 197–207.

[6] S. M. Faruque, I. B. Naser, M. J. Islam, A. S. G. Faruque, A. N. Ghosh, G. B. Nair, D. A. Sack and J. J. Mekalanos, Seasonal epidemics of cholera inversely correlate with the prevalence of environmental cholera phages, *Proc. Nat. Acad. Sci.,* **102** (2004), 1702–1707.

[7] J. K. Hale, *Ordinary Differential Equations*, Pure and Applied Mathematics, Vol. XXI, Wiley-Interscience, New York, 1969.

[8] D. M. Hartley, J. G. Morris and D. L. Smith, Hyperinfectivity: A critical element in the ability of V. cholerae to cause epidemics?, *PLoS Medicine*, **3** (2006), e7.

[9] M. A. Jensen, S. M. Faruque, J. J. Mekalanos and B. R. levin, Modeling the role of bacteriophage in the control of cholera outbreaks, *PNAS*, **103** (2006), 4652–4657.
[10] R. I. Joh, H. Wang, H. Weiss and J. S. Weitz, Dynamics of indirectly transmitted infectious diseases with immunological threshold, *Bull. Math. Bio.,* **71** (2009), 845–862.
[11] J. D. Kong, W. Davis, X. Li and H. Wang, Stability and sensitivity analysis of the iSIR model for indirectly transmitted infectious dieases with immunological threshold, *SIAM J. Appl. Math.*, **74** (2014), 1418–1441.
[12] S. Liao and J. Wang, Stability analysis and application of a mathematical cholera model, *Math. Biosci. and Eng.*, **8** (2011), 733–752.
[13] Z. Mukandavire, S. Liao, J. Wang, H. Gaff, D. L. Smith and J. G. Morris Jr., Estimating the reproductive numbers for the 2008-2009 cholera outbreaks in Zimbabwe, *Proc. Nat. Acad. Sci.,* **108** (2011), 8767–8772.
[14] E. J. Nelson, J. B. Harris, J. G. Morris, S. B. Calderwood and A. Camilli, Cholera transmission: The host, pathogen and bacteriophage dynamics, *Nature Reviews: Microbiology*, **7** (2009), 693–702.
[15] L. Righetto, E. Bertuzzo, L. Mari, E. Schild, R. Casagrandi, M. Gatto, I. Rodriguez-Iturbe and A. Rinaldo, Rainfall mediations in the spreading of epidemic cholera, *Advances in Water Resources*, **60** (2013), 34–46.
[16] L. Righetto, R. Casagrandi, E. Bertuzzo, L. Mari, M. Gatto, I. Rodriguez-Iturbe and A. Rinaldo, The role of aquatic reservoir fluctuations in long-term cholera patterns, *Epidemics*, **4** (2012), 33–42.
[17] F. L. Thompson, B. Austin and J. Swings, *The Biology of Vibrios*, ASM Press, Washington, D.C., 2006.
[18] J. P. Tian and J. Wang, Global stability for cholera epidemic models, *Math. Biosci.,* **232** (2011), 31–41.
[19] J. H. Tien and D. J. D. Earn, Multiple transmission pathways and disease dynamics in a waterborne pathogen model, *Bull. Math. Bio.*, **72** (2010), 1502–1533.
[20] A. L. Tuite, J. Tien, M. Eisenberg, D. J. D. Earn, J. Ma and D. N. Fisman, Cholera epidemic in Haiti, 2010: Using a transmission model to explain spatial spread of disease and identify optimal control interventions, *Ann. Intern. Med.*, **154** (2011), 593–601.
[21] F. Verhulst, *Nonlinear Differential Equations and Dynamical Systems*, Second Edition, Springer, Berlin, 1996.
[22] J. Wang and S. Liao, A generalized cholera model and epidemic-endemic analysis, *J. Biol. Dyn.,* **6** (2012), 568–589.
[23] T. Yoshizawa, *Stability Theory and the Existence of Periodic Solutions and Almost Periodic Solutins*, Appl. Math. Science, Vol.14, Springer-Verlag, 1975.
[24] World Health Organization (WHO) web page: `http://www.who.org`.

Received March 2015; revised January 2017.

E-mail address: `jhluo@shou.edu.cn`
E-mail address: `Jin-Wang02@utc.edu`
E-mail address: `hao8@ualberta.ca`